

# Representation of the Joystick Using the Virtual Configuration

Hiroki Kato<sup>a</sup> and Masamitsu Kurisu<sup>a</sup>

<sup>a</sup>Department of Mechanical Engineering, Tokyo Denki University, Japan  
E-mail: 17kkm04@ms.dendai.ac.jp, kurisu@cck.dendai.ac.jp

## Abstract -

Recently, facilities that are a foundation of industries such as roads, water pipes, and tunnels are getting old. Along with this, the demand on inspection in the decrepit facilities is increasing. The robots are introduced to inspection in these facilities. It is required that the operators can control the robots easily when facilities are inspected using the robots. However, the control device which the operators can operate the robots easily is different depending on the robots which are controlled and the inspection task. Therefore, a control device which enables us to control various robots is developed by us. The device can represent various operation manners by changing the shape. In this paper, a method of device control with a virtual configuration is described. A joystick is represented using the virtual configuration. The torques to be outputted to each joint of the joystick are calculated using the forces and moments which applied to the grip of the device by the operators. The calculated forces and torques are distributed to the torques which drive each joint in the device. Therefore, the joystick using the virtual configuration is represented. The usability of the proposed method is shown by verification experiments.

## Keywords -

Virtual configuration; Remote operation; Control device;

## 1 Introduction

Recently, facilities that are the foundation of industries such as roads, water pipes, and tunnels are getting old. In this paper, these facilities are called the social infrastructures from now on. The demand on inspection in the social infrastructures are increasing along with the increase of the decrepit social infrastructure. There are many scenes where a judgment by humans is required in the inspection task of the social infrastructures. However, there are some situations that are difficult for humans to enter depending on the environment where the inspection task is performed. Therefore, it is desired to assist the inspection task is performed by humans with controlling the robots remotely. Against this backdrop, development and introduction of next generation robots for the social infrastructures are done in Japan since 2013[1]. On the other hand, the number of experts who inspect the social

infrastructures is decreasing. Therefore, it is demanded to inspect efficiently even if an operator is not used to controlling the robots. Various robots which inspect the social infrastructures is developed[2][3]. Also, a hexapod robot for inspection in narrow environment is developed by us[4]. It is required that the operators can control the robots easily when the social infrastructures are inspected using these robots. On the other hand, a control device and an operation manner are different depending on the robots which are controlled and the inspection task.

A cockpit and a control device which enables us to control various robots are developed by us (Figure 1). The control device has a virtual configuration represented by using a multiple virtual axes of rotation. A virtual axis of rotation which does not exist in the actual configuration is represented by combining multiple axis of rotation as shown in Figure 2. In this paper, a representation of a joystick using the virtual configuration is described. Hereinafter, The joystick which is represented using the virtual configuration is called the virtual joystick.

Overview of the virtual axis of rotation is described. In the case of the actual axis of rotation, the moments applied to the axis of rotation can be divided into a moment about the axis of rotation and others. Object rotates about



Figure 1. The cockpit which is developed by us.

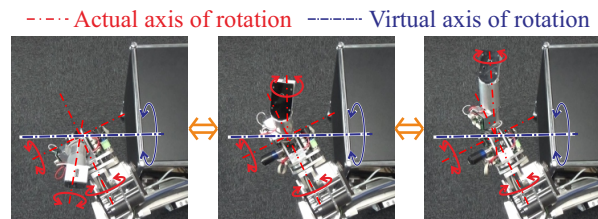


Figure 2. The actual axis of rotation and the virtual axis of rotation.

the axis of rotation by the moment about the axis of rotation. Hereafter, the moment about the axis of rotation is called the unconstrained force. On the other hand, the moments and forces other than the unconstrained force applied to the axis of rotation is received by the structure of the axis of rotation. The forces which received the moments and forces by the structure of the axis of rotation is called the mechanically constrained forces from now on. However, in the case of the virtual axis of rotation, the mechanically constrained forces cannot be achieved by the structure of axis of rotation. Therefore, the mechanically constrained forces are achieved by position control if the virtual axis of rotation is represented. On the other hand, control to achieve the mechanical behavior which want to be represented is performed about unconstrained force. The virtual axis of rotation is represented by the unconstrained force and the mechanically constrained forces. The unconstrained force is a spring force if the joystick is represented. The representation of the virtual axis of rotation is performed as follows. First, a coordinate system of the virtual axis of rotation  $\Sigma_V$  is fixed at a position where the virtual axis of rotation is represented. Then, the unconstrained force and the mechanically constrained forces required to represent the virtual axis of rotation are calculated. The unconstrained force and the mechanically constrained forces are represented by the forces which in each coordinate axis direction in  $\Sigma_V$  and the torques which about each coordinate axis in  $\Sigma_V$  to be outputted to  $\Sigma_V$ . The forces and torques are distributed to the torques which drive each joint in the device. The virtual axis of rotation is represented by the torques which drive each joint in the device.

The structure of this paper is as follows. First, related work is described in section 2. The control device which is developed by us is described in section 3. The methods of representing the virtual joystick and the virtual axis of rotation are described at the beginning of section 4. Then, the method of calculating the forces and torques to be outputted to  $\Sigma_V$  using the forces applied to the grip of the control device by the operators is indicated. The method of distributing the calculated forces and torques to the torques which drive each joint in the actual device is shown at the end of section 4. The usability of the proposed method is shown by verification experiments in section 5. Finally, conclusion is described in section 6.

## 2 Related Work

A lot of devices for controlling robots are studied. An equipment for controlling a mobile robot is developed by Yamazawa et al.[5]. Locomotion interface and immersive projection display are used in the equipment. The robot is controlled using the walking information of a operator. A cockpit for controlling humanoids is devel-

oped by Tachi et al.[6]. An equipment for controlling humanoids in the cockpit has the same configuration as the arm of humanoids. Humanoids are controlled by using the master-slave control system. These equipment enables us to control the robots intuitively. However, these equipment has only one operation target. Using a motion capture to control humanoids is studied. A system that control humanoids using optical motion capture is developed by Kurihara et al.[7]. Using the motion capture enables us to control humanoids intuitively. However, the equipment becomes large scale in the case of using motion capture. Hull which is a cockpit for controlling robots is developed by Institute Future Robotics Technology Center, Chiba Institute of Technology [8]. Hull has haptic interface. It is able to present the forces applied to the robot to the operator by using the haptic interface. Bilateral master-slave control is proposed for force feedback control to the operators[9][10] [11]. Among them, a bilateral master-slave control with different configuration is proposed by Arai et al.[12]. It is possible to combine the slave with high workability and the master with high operability by using the proposed method in document [12]. Further, there is an advantage that general versatility is enhanced and modularization is easy to perform. The master is given the torque which drive each joint of the master as the commanded value in the bilateral master-slave control with different configuration. Applying the bilateral master-slave control with different configuration to the device which is developed by us is considering.

## 3 The Control Device Which is Developed by Us

The control device which enables us to control various robots is developed by us. The device is shown in Figure 3. The device is composed with one prismatic joint and five revolute joints. A DC motor and a rotary encoder are installed on each joint to use the device as a haptic interface. An angle of each joint is acquired by the rotary encoder. A 6-axis force sensor is installed between 5th axis and 6th axis of the device. It is possible to measure the forces and moments which applied to the grip of the device by the operators using the force sensor.

The device can represent various operation manners by changing the shape. The operation manners that can be represented at present is shown in Figure 4. Joystick Mode in Figure 4(a) is a mode that represents a joystick on the market. 3D Input Mode in Figure 4(b) is a mode that represents the gaming device “Falcon” sold by Novint company. Any point on the three-dimensional space can be designated by 3D Input Mode. Dedicated Input Mode in Figure 4(c) is a mode exclusive to the hexapod robot which is developed by us. The configuration of the device in Dedicated Input Mode is the same as that of a limb of

the hexapod robot. Therefore, it is possible to perform an intuitive control like actually grasping the limb of hexapod robot. Please refer to document [4] for details of the hexapod robot.

## 4 Representation of the Joystick Using the Virtual Configuration.

### 4.1 The Virtual Joystick

The control device which is developed by us can be represented various operation manners by changing the shape. However, the movable axes installed on the actual device may not be orthogonal in some cases. In that case, it cannot represent the joystick by using only axes of rotation installed on the device. Therefore, the virtual axis of

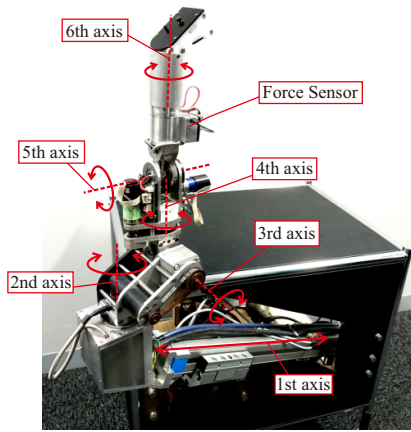


Figure 3. The control device which is developed by us.

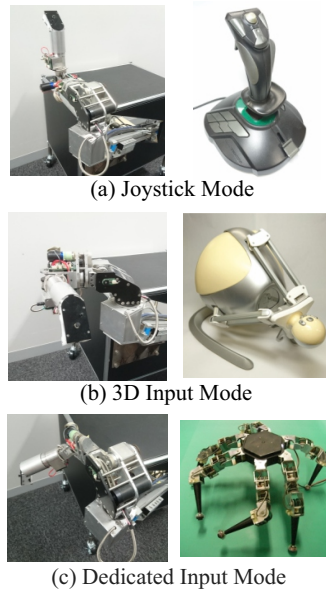


Figure 4. The operation manners that can be represented at present.

rotation different from the actual axis of rotation as shown in Figure 2 is used. The joystick is represented using three virtual axes of rotation orthogonal to one another. The method of representing the virtual joystick is described below. First, a coordinate system of the virtual axis of rotation is fixed newly at a position where the virtual axis of rotation is represented as shown in Figure 5. The coordinate system is denoted as  $\Sigma_V$ . One of the coordinate axes in  $\Sigma_V$  is made to overlap with the virtual axis of rotation. In this example,  $Y$ -axis in  $\Sigma_V$  is made to overlap the virtual axis of rotation. The position of  $\Sigma_V$  is fixed. Further, only rotation about  $Y$ -axis in  $\Sigma_V$  is performed, thereby the virtual axis of rotation is represented.

The forces in each coordinate axis direction in  $\Sigma_V$  to be outputted to  $\Sigma_V$  is denoted as  ${}^V\mathbf{f}_v = [{}^Vf_x, {}^Vf_y, {}^Vf_z]^T$ . The torques about each coordinate axis in  $\Sigma_V$  to be outputted to  $\Sigma_V$  is denoted as  ${}^V\boldsymbol{\tau}_v = [{}^V\tau_x, {}^V\tau_y, {}^V\tau_z]^T$ . The unconstrained force and the mechanically constrained forces for representing the virtual axis of rotation are represented by  ${}^V\mathbf{f}_v$  and  ${}^V\boldsymbol{\tau}_v$ . In this example, only rotation about the  $Y$ -axis in  $\Sigma_V$  is performed. Therefore,  ${}^V\tau_x$ ,  ${}^V\tau_z$ , and  ${}^Vf_v$  are the mechanically constrained forces. Also,  ${}^V\tau_y$  is the unconstrained force. Since the joystick is represented this time, the unconstrained force is spring force. Also, the mechanically constrained forces are represented by position control.  ${}^V\mathbf{f}_v$  and  ${}^V\boldsymbol{\tau}_v$  are calculated using the forces and moments which applied to the grip of the device by the operators. It is impossible to directly output  ${}^V\mathbf{f}_v$  and  ${}^V\boldsymbol{\tau}_v$  to the virtual axis of rotation because the virtual axis of rotation does not exist in the actual configuration of the device.  ${}^V\mathbf{f}_v$  and  ${}^V\boldsymbol{\tau}_v$  are distributed to the torques which drive each joint in the device. The equilibrium of the force and moment in static mechanics is used for the distribution. The details are described below.

### 4.2 Each Coordinate System Used for Calculation.

Each coordinate system used for calculation is as follows. The coordinate systems of each joint and the force sensor are assigned as shown in Figure 6. A world coordinate system is denoted as  $\Sigma_W$ . The positive direction of

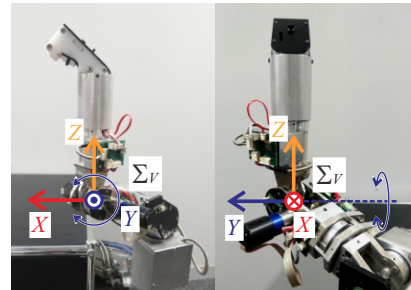


Figure 5. The position where the coordinate system of the virtual axis of rotation is fixed.

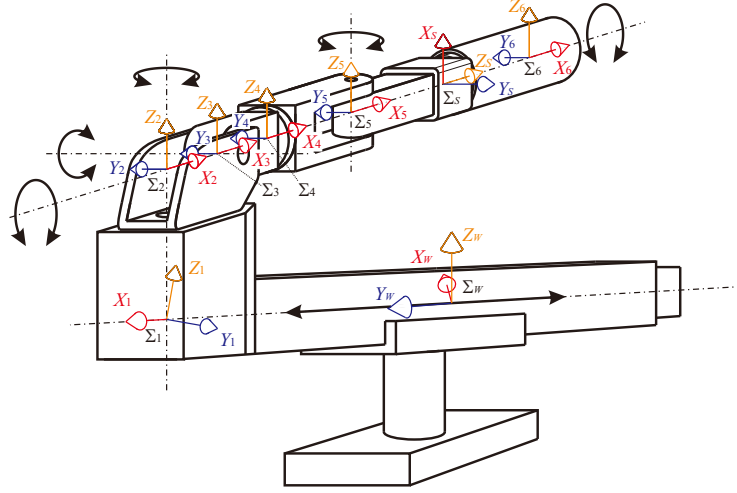


Figure 6. The position where each coordinate system is fixed on the device.

the  $X$ -axis in  $\Sigma_W$  is assigned in the same direction as the front direction of the operator. Also, the positive direction of the  $Z$ -axis in  $\Sigma_W$  is assigned as the upward direction perpendicular to the ground. The coordinate system of  $i$ -th axis is denoted as  $\Sigma_i (i = 1, 2, \dots, 6)$ .  $\Sigma_1$  is fixed at the intersection of 1st axis and 2nd axis. The  $X$ -axis in  $\Sigma_1$  is the same direction as a movable axis of the prismatic joint. All  $\Sigma_i (i = 2, 3, \dots, 6)$  are the same posture in the case of the device is the initial posture. A coordinate system of the 6-axis force sensor is denoted as  $\Sigma_S$ . The origin of  $\Sigma_V$  is fixed to the same position as the origin of  $\Sigma_5$  at this time. Also, the initial posture of  $\Sigma_V$  is the same as that of  $\Sigma_W$ .

#### 4.3 Calculations of the Forces and Torques to Be Outputted to $\Sigma_V$ .

${}^V f_v$  is outputted to the origin of  $\Sigma_V$  as the mechanically constrained forces. Since the mechanically constrained forces are achieved by position control,  ${}^V f_v$  is calculated using Equation(1).

$${}^V f_v = -K_p \Delta p + K_d(\mathbf{0} - \dot{p}) \quad (1)$$

${}^V f_v (\in R^{3 \times 1})$ : The forces in  $X$ -axis,  $Y$ -axis, and  $Z$ -axis direction in  $\Sigma_V$  to be outputted to the origin of  $\Sigma_V$  [N].

$K_p (\in R^{3 \times 3})$ : Proportional gain matrix.

$\Delta p (\in R^{3 \times 1})$ : Deviations of Position in  $X$ -axis,  $Y$ -axis, and  $Z$ -axis direction in  $\Sigma_V$  from the initial position of the origin of  $\Sigma_V$  [m].

$K_d (\in R^{3 \times 3})$ : Differential gain matrix.

${}^V \tau_v = [{}^V \tau_x, {}^V \tau_y, {}^V \tau_z]^T$  are calculated as follows. Since  ${}^V \tau_x$  and  ${}^V \tau_z$  are the mechanically constrained forces, these are achieved by position control in the same way as  ${}^V f_v$ . Therefore,  ${}^V \tau_x$  and  ${}^V \tau_z$  are calculated using Equation(2).

$${}^V \tau_i = -k_p \Delta q_i + k_d(0 - \dot{q}_i) \quad (i = x, z) \quad (2)$$

${}^V \tau_i$ : The torque about  $i$ -axis in  $\Sigma_V$  to be outputted to  $\Sigma_V$  [N·m] ( $i = x, z$ ).

$k_p$ : Proportional gain.

$\Delta q_i$ : Angular displacement about  $i$ -axis in  $\Sigma_V$  [rad] ( $i = x, z$ ).

$k_d$ : Differential gain.

On the other hand,  ${}^V \tau_y$  is the unconstrained force. Since the joystick is represented by using the virtual axis, the unconstrained force is spring force. Therefore,  ${}^V \tau_y$  is calculated using Equation(3). The forces and moments which applied to the grip of the device by the operators acquired from the force sensor are used for the calculations.

$${}^V \tau_y = {}^V F_x l - k_{pj} \Delta q_y \quad (3)$$

${}^V \tau_y$ : The torque about  $Y$ -axis in  $\Sigma_V$  to be outputted to  $\Sigma_V$  [N·m].

${}^V F_x$ : The force in  $X$ -axis direction in  $\Sigma_V$  applied to grip of the device by the operators [N].

$l$ : Length from the origin of  $\Sigma_S$  to the origin of  $\Sigma_V$  [m].

$k_{pj}$ : Proportional gain used for representation of the joystick.

$\Delta q_y$ : Angular displacement about  $Y$ -axis in  $\Sigma_V$  [rad].

It is possible to represent the virtual axis of rotation about the  $X$ -axis in  $\Sigma_V$  by using Equation(4) instead of Equation(3). Also, it is possible to represent the virtual axis of rotation about the  $Z$ -axis in  $\Sigma_V$  by using Equation(5) instead of Equation(3). In that case,  ${}^V \tau_y$  is calculated using Equation(2) as  $i = y$ .

$${}^V \tau_x = -{}^V F_y l - k_{pj} \Delta q_x \quad (4)$$

$${}^V \tau_z = {}^V M_z - k_{pj} \Delta q_z \quad (5)$$

${}^V\tau_i$ : The torque about  $i$ -axis in  $\Sigma_V$  to be outputted to  $\Sigma_V$ [N·m] ( $i = x, z$ ).

${}^V F_y$ : The force in  $Y$ -axis direction in  $\Sigma_V$  applied to grip of the device by the operators[N].

${}^V M_z$ : The moment about  $Z$ -axis direction in  $\Sigma_V$  applied to grip of the device by the operators[N·m].

$l$ : Length from the origin of  $\Sigma_S$  to the origin of  $\Sigma_V$ [m].

$k_{pj}$ : Proportional gain used for representation of the joystick.

$\Delta q_i$ : Angular displacement about  $i$ -axis in  $\Sigma_V$ [rad] ( $i = x, z$ ).

#### 4.4 Calculation of the Angular Displacement About Each Coordinate Axis in $\Sigma_V$ .

The angular displacement about each coordinate axis in  $\Sigma_V$  are necessary to calculate  ${}^V\tau_v$  using Equation(2)-(5). However, the virtual configuration is different from the actual configuration. Therefore, the angular displacement cannot be gotten directly using the rotary encoder installed on each joint of the device. The calculations of the angular displacement about each coordinate axis in  $\Sigma_V$  are performed as follows.

A initial coordinate system of the virtual axis of rotation is denoted as  $\Sigma_{V_0}$ . It is supposed that  $\Sigma_{V_0}$  becomes  $\Sigma_V$  by operating the device. The positions of the origin of  $\Sigma_{V_0}$  and  $\Sigma_V$  don't be changed. It is supposed that  ${}^{V_0}\mathbf{R}_V$  can be calculated by forward kinematics at this time. A rotation matrix from  $\Sigma_{V_0}$  to  $\Sigma_V$  is denoted as  ${}^{V_0}\mathbf{R}_V$ . Then,  ${}^{V_0}\mathbf{R}_V$  is expressed by Equation(6) using  $R_{ij}$  ( $i, j = 1, 2, 3$ ) that are known parameters.

$${}^{V_0}\mathbf{R}_V = \begin{bmatrix} R_{11} & R_{12} & R_{13} \\ R_{21} & R_{22} & R_{23} \\ R_{31} & R_{32} & R_{33} \end{bmatrix} \quad (6)$$

On the other hand, the angular displacement about each coordinate axis in  $\Sigma_V$  can be represented by the roll, pitch, and yaw angles because the joystick is represented. Therefore, the rotation matrix can be calculated using a representation by the roll, pitch, and yaw angles. The roll, pitch, and yaw angles are denoted as  $\phi$ ,  $\theta$ , and  $\psi$ . The rotation matrix  ${}^{V_0}\mathbf{R}_V$  from  $\Sigma_{V_0}$  to  $\Sigma_V$  is given by Equation(7) using  $\phi$ ,  $\theta$ , and  $\psi$ .

$${}^{V_0}\mathbf{R}_V = \begin{bmatrix} C_\theta C_\psi & -C_\theta S_\psi + S_\phi S_\theta C_\psi & S_\theta S_\psi + C_\phi S_\theta C_\psi \\ C_\theta S_\psi & C_\theta C_\psi + S_\phi S_\theta S_\psi & -S_\phi C_\psi + C_\phi S_\theta S_\psi \\ -S_\theta & S_\phi C_\theta & C_\phi C_\theta \end{bmatrix} \quad (7)$$

Here,  $S_\phi = \sin\phi$  and  $C_\phi = \cos\phi$ . The same applies to  $\theta$

and  $\psi$ . Equation(8) is obtained from Equation(6) and (7).

$$\begin{cases} \text{if } \sin(\theta) = 1 & \begin{cases} \phi = 0 \\ \theta = \frac{\pi}{2} \\ \psi = \text{atan2}(R_{23}, R_{22}) \end{cases} \\ \text{if } \sin(\theta) = -1 & \begin{cases} \phi = 0 \\ \theta = -\frac{\pi}{2} \\ \psi = -\text{atan2}(R_{23}, R_{22}) \end{cases} \\ \text{otherwise} & \begin{cases} \phi = \text{atan2}(R_{32}, R_{33}) \\ \theta = -\text{asin}(R_{31}) \\ \psi = \text{atan2}(R_{21}, R_{11}) \end{cases} \end{cases} \quad (8)$$

However, the values of  $\phi$  and  $\psi$  can not be uniquely decided in the case of  $\sin(\theta) = \pm 1$ . In this case, it is assumed that  $\phi = 0$ . From the above,  $\phi$ ,  $\theta$ , and  $\psi$  are calculated.

For example, the case of applying to the our device is described.  $\Sigma_{V_0}$  is fixed by us so that the postures of  $\Sigma_{V_0}$  and  $\Sigma_W$  are the same. Therefore,  ${}^{V_0}\mathbf{R}_V$  can be expressed as Equation(9).

$${}^{V_0}\mathbf{R}_V = {}^W\mathbf{R}_V = {}^W\mathbf{R}_6 {}^6\mathbf{R}_V \quad (9)$$

Here, a rotation matrix from  $\Sigma_W$  to  $\Sigma_6$  is denoted as  ${}^W\mathbf{R}_6$ . A rotation matrix from  $\Sigma_6$  to  $\Sigma_V$  is denoted as  ${}^6\mathbf{R}_V$ .  $\Sigma_V$  always follows the movement of  $\Sigma_6$ . Also, the posture of  $\Sigma_6$  becomes the same as that of  $\Sigma_V$  when rotated only  $\pi/2$  about  $Y$ -axis in  $\Sigma_6$ . Therefore,  ${}^6\mathbf{R}_V$  is always given by Equation(10).

$${}^6\mathbf{R}_V = \begin{bmatrix} \cos(\pi/2) & 0 & \sin(\pi/2) \\ 0 & 1 & 0 \\ -\sin(\pi/2) & 0 & \cos(\pi/2) \end{bmatrix} = \begin{bmatrix} 0 & 0 & 1 \\ 0 & 1 & 0 \\ -1 & 0 & 0 \end{bmatrix} \quad (10)$$

On the other hand,  ${}^W\mathbf{R}_6$  can be calculated by using forward kinematics, thereby  $R_{ij}$  ( $i, j = 1, 2, 3$ ) in Equation(6) are obtained.  $\phi$ ,  $\theta$ , and  $\psi$  are calculated using  $R_{ij}$  ( $i, j = 1, 2, 3$ ) and Equation(8).

#### 4.5 Distribution of the Calculated Forces and Torques to the Torques Which Drive Each Joint in the Device.

In this section, the method of distributing  ${}^V\mathbf{f}_v$  and  ${}^V\tau_v$  to the torques which drive each joint in the device is described. The same idea as calculations of the each joint torques which are balanced with the forces and moments applied to the end effector in the robot manipulators is used[13].  ${}^V\mathbf{f}_v$  corresponds to the forces which applied to the end effector of the robot manipulators. Also,  ${}^V\tau_v$  corresponds to the moments which applied to the end effector of the robot manipulators. The each joint torques which are balanced with the forces and moments applied

to the end effector are calculated in the case of a robot manipulators. However,  ${}^V\mathbf{f}_v$  and  ${}^V\boldsymbol{\tau}_v$  are outputted to  $\Sigma_V$  by using the torques which drive each joint in the device in the case of the virtual axis of rotation. Therefore, keep in mind that signs are different when calculating the torques of the robot manipulators and the virtual configuration.

${}^V\mathbf{f}_v$  and  ${}^V\boldsymbol{\tau}_v$  which are calculated using Equation(1)-(5) are the forces and torques expressed in  $\Sigma_V$ .  ${}^W\mathbf{f}_v$  and  ${}^W\boldsymbol{\tau}_v$  which are  ${}^V\mathbf{f}_v$  and  ${}^V\boldsymbol{\tau}_v$  expressed in  $\Sigma_W$  are given by Equation(11) and (12) by the equilibrium of force and moment in static mechanics.

$${}^W\mathbf{f}_v = {}^W\mathbf{R}_V {}^V\mathbf{f}_v \quad (11)$$

$${}^W\boldsymbol{\tau}_v = {}^W\mathbf{R}_V {}^V\boldsymbol{\tau}_v + {}^W\mathbf{p}_V \times ({}^W\mathbf{R}_V {}^V\mathbf{f}_v) \quad (12)$$

The position vector of  $\Sigma_V$  expressed in  $\Sigma_W$  is denoted as  ${}^W\mathbf{p}_V$ . Cross product of vectors is denoted as “ $\times$ ”.  ${}^W\mathbf{p}_V = [{}^Wp_x, {}^Wp_y, {}^Wp_z]^T$  and Equation(13) are defined by us.

$$[{}^W\mathbf{p}_V \times] = \begin{bmatrix} 0 & -{}^Wp_z & {}^Wp_y \\ {}^Wp_z & 0 & -{}^Wp_x \\ -{}^Wp_y & {}^Wp_x & 0 \end{bmatrix} \quad (13)$$

Accordingly, Equation(11) and (12) are expressed by Equation(14).

$$\begin{bmatrix} {}^W\mathbf{f}_v \\ {}^W\boldsymbol{\tau}_v \end{bmatrix} = \begin{bmatrix} {}^W\mathbf{R}_V & \mathbf{0} \\ [{}^W\mathbf{p}_V \times] {}^W\mathbf{R}_V & {}^W\mathbf{R}_V \end{bmatrix} \begin{bmatrix} {}^V\mathbf{f}_v \\ {}^V\boldsymbol{\tau}_v \end{bmatrix} \quad (14)$$

The relationship between the torques which drive each joint  $\boldsymbol{\tau} (\in R^{6 \times 1})$ ,  ${}^W\mathbf{f}_v$ , and  ${}^W\boldsymbol{\tau}_v$  is expressed by Equation(15) using Jacobian matrix  $\mathbf{J} (\in R^{6 \times 6})$ .

$$\boldsymbol{\tau} = -\mathbf{J}^T \begin{bmatrix} {}^W\mathbf{f}_v \\ {}^W\boldsymbol{\tau}_v \end{bmatrix} \quad (15)$$

Therefore, the relationship between  ${}^V\mathbf{f}_v$ ,  ${}^V\boldsymbol{\tau}_v$ , and  $\boldsymbol{\tau}$  is expressed by Equation(16) from Equation(14) and (15).

$$\boldsymbol{\tau} = -\mathbf{J}^T \begin{bmatrix} {}^W\mathbf{R}_V & \mathbf{0} \\ [{}^W\mathbf{p}_V \times] {}^W\mathbf{R}_V & {}^W\mathbf{R}_V \end{bmatrix} \begin{bmatrix} {}^V\mathbf{f}_v \\ {}^V\boldsymbol{\tau}_v \end{bmatrix} \quad (16)$$

${}^V\mathbf{f}_v$  and  ${}^V\boldsymbol{\tau}_v$  are distributed to the torques which drive each joint in the actual device using Equation(16).

## 5 Verification Experiments

### 5.1 The Representation of the Virtual Joystick

An experiment is performed, thereby it is confirmed that the virtual joystick is represented by using the proposed method. The joystick with one virtual axis of rotation is represented in the experiment. The virtual axis of rotation is installed as shown in Figure 7. The forces in lateral direction and longitudinal direction against the virtual axis

of rotation are applied to the grip of the device and a behavior of the device is observed. The spring scale is used to understand easily and visually the forces that applied to the grip of the device. Measurable range of the spring scale is 0 to 2 kgf. The behavior of the device in the case of the virtual axis of rotation is not represented is also observed for purposes of comparison. The device is only performed gravity compensation when the virtual axis of rotation is not represented.

The top-view of the device is shown in Figure 8 as the experiment result. The result in the case of performing only gravity compensation without the virtual axis of rotation is indicated by a red frame in Figure 8. Also, the result in the case of the virtual axis of rotation is represented is indicated by a blue frame in Figure 8. Small red triangles are put in Figure 8 in order to easily understand elongation of the spring scale. The grip of the device should move on the red dashed line in Figure 8 if the virtual axis is installed as shown in Figure 7.

The grip of the device is leaning in the direction to which the forces were applied in the case of the virtual axis of rotation was not represented. And the grip of the device is moving away from the red dashed line. On the other hand, the following results were obtained in the case of the virtual axis of rotation was represented. The grip is rotating about the virtual axis of rotation when the forces were applied in lateral direction against the virtual axis of rotation. And the grip of the device is moving on the red dashed line. Also, it is confirmed by looking at the spring scale that the forces applied to the grip of the device are increasing as angular displacement from initial posture is increasing. The grip is not leaning even if the forces which applied to the grip increased when the forces were applied in lateral direction against the virtual axis of rotation. From the above results, it is considered that the virtual joystick has been represented by using the proposed method.

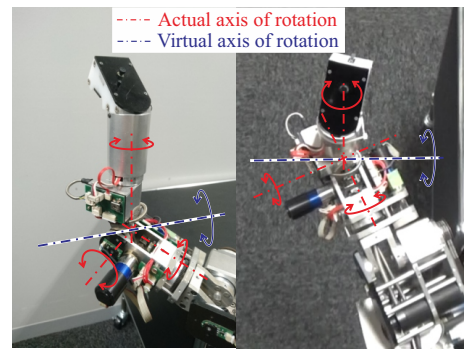


Figure 7. The place where the virtual axis of rotation is installed.

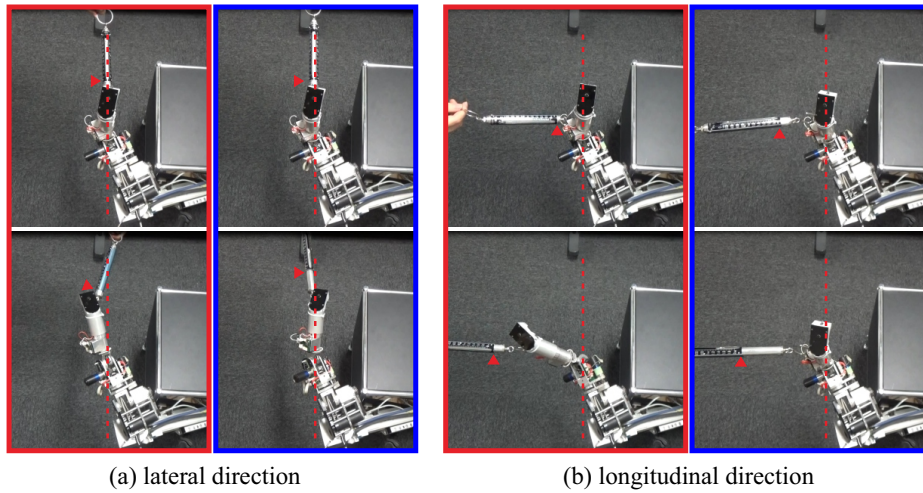


Figure 8. The behavior of the device when forces are applied in lateral direction and longitudinal direction against the virtual axis of rotation (Red frame: Without virtual axis of rotation, Blue frame: With virtual axis of rotation).

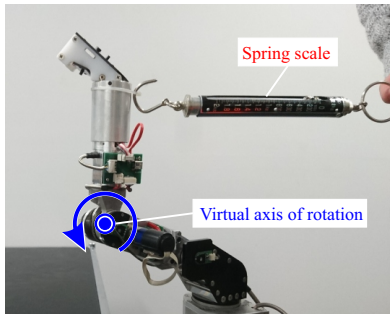


Figure 9. The environment in which the experiment is performed.

### 5.2 The Torques Outputted to the Virtual Axis of Rotation.

The torques to be outputted to the virtual axis of rotation are distributed to the torques which drive each joint in the device by using Equation(16). A experiment is performed, thereby it is confirmed whether the required torques are actually outputted to the virtual axis of rotation by the torques which drive each joint in the device. The experiment is performed as follows. The environment in which the experiment is performed is shown in Figure 9. A commanded torques to the virtual axis of rotation are given. The commanded torques are distributed to the torques which drive each joint in the device by using Equation(16). The forces outputted to the grip of the device at this time are measured using the spring scale. The torques actually being outputted to the virtual axis of rotation are calculated. The measured values of the forces and the distance from the point where the forces were measured to the virtual axis of rotation are used for the calculation. The measured values of torques and the commanded values of torques are compared. 1.0, 1.2, 1.4, 1.6, 1.8, and 2.0 N are

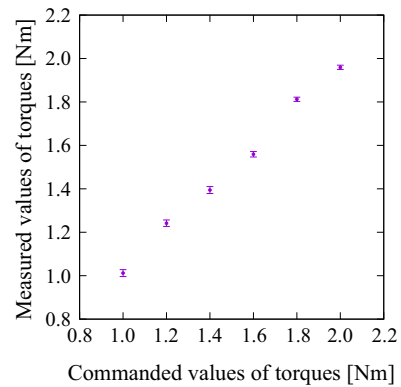


Figure 10. The relationship between the commanded values of torques and the measured values of torques.

given five times respectively as the commanded torque.

The relationship between the commanded values of torques and the measured values of torques obtained from the experiment is shown in Figure 10. The horizontal line is the commanded values of torques, and the vertical line is the measured values of torques. The points are the mean values of the measured values of torques. The error bars are standard deviation. Figure 10 shows that the ratio between the commanded values of torques and the measured values of torques is about 1 : 1. Also, the standard deviation is small. Therefore, it is considered that the required torques are actually outputted to the virtual axis of rotation by the torques which drive each joint in the device.

The above results show that it is possible to output the torques commanded by us to the virtual axis of rotation. Therefore, it is considered that the bilateral master-slave control with different configuration proposed in document [12] can be applied to the device with the virtual configuration.

## 6 Conclusion

In this paper, the representation of the joystick using the virtual configuration was described. The coordinate system of the virtual axis of rotation was fixed. The virtual axis of rotation was represented with performing only rotation about one coordinate axis of the coordinate system. The method of calculating the forces and torques to be outputted to the coordinate system using the forces moments applied to the grip of the control device by the operators was shown. Then, the method for obtain the angular displacement about each coordinate axis in the coordinate system required for the calculations of the forces and torques was shown. In addition, the method of distributing the calculated forces and torques to the torques which drive each joint in the device was shown. The virtual axis of rotation was represented using the above methods. Finally, the usability of the proposed method was verified by performing the verification experiments.

On the other hand, there are two problems in the proposed method. First, the equation in static mechanics is used when the forces and torques are distributed. Therefore, the movement with large inertial force is not considered. Then, the virtual axis of rotation was represented in only one position. It is thought that the representation of more operation manners becomes possible by representing virtual axes of rotation at multiple position. The future task of this study is to deal with these problems and further extend the representation of the control device with the virtual configuration.

## References

- [1] Advanced Construction Technology Center. Next-generation robotic technologies for social infrastructure-robotic system~field demonstration portal site~. On-line: <https://www.c-robotech.info/>, Accessed: 3/1/2018.
- [2] N Gucunski, S-H Kee, H La, B Basily, A Maher, and H Ghasemi. Implementation of a fully autonomous platform for assessment of concrete bridge decks rabbit. In *Structures Congress 2015*, pages 367–378, 2015.
- [3] Mitsubishi Heavy Industries. Joint development of japan's first anti-explosive remotely operated mobile robot contributing to safe and efficient data collection and inspection in tunnel accidents and petrochemical plants. On-line: <http://www.mhi.com/news/story/160712.html>, Accessed: 3/1/2018.
- [4] Masamitsu Kurisu. A study on teleoperation system for a hexapod robot-development of a prototype platform. In *Mechatronics and Automation (ICMA), 2011 International Conference on*, pages 135–141. IEEE, 2011.
- [5] Kazumasa Yamazawa, Masaki Tawada, and Naokazu Yokoya. Remote control of a networked mobile robot using an immersive locomotion interface. In *Multi-media and Expo, 2006 IEEE International Conference on*, pages 2117–2120. IEEE, 2006.
- [6] Susumu Tachi, Kiyoshi Komoriya, Kazuya Sawada, Takashi Nishiyama, Toshiyuki Itoko, Masami Kobayashi, and Kozo Inoue. Telexistence cockpit for humanoid robot control. *Advanced Robotics*, 17(3):199–217, 2003.
- [7] Kazutaka Kurihara, Shin'ichiro Hoshino, Katsu Yamane, and Yoshihiko Nakamura. Optical motion capture system with pan-tilt camera tracking and real time data processing. In *Robotics and Automation, 2002. Proceedings. ICRA'02. IEEE International Conference on*, volume 2, pages 1241–1248. IEEE, 2002.
- [8] Chiba Institute of Technology. Hull:a cockpit system. On-line: <http://www.furo.org/en/works/hull/hull.html>, Accessed: 5/1/2018.
- [9] Robert J Anderson and Mark W Spong. Bilateral control of teleoperators with time delay. *IEEE Transactions on Automatic control*, 34(5):494–501, 1989.
- [10] Yasuyoshi Yokokohji and Tsuneo Yoshikawa. Bilateral control of master-slave manipulators for ideal kinesthetic coupling-formulation and experiment. *IEEE transactions on robotics and automation*, 10(5):605–620, 1994.
- [11] Jee-Hwan Ryu and Dong-Soo Kwon. A novel adaptive bilateral control scheme using similar closed-loop dynamic characteristics of master/slave manipulators. *Journal of Field Robotics*, 18(9):533–543, 2001.
- [12] Arai Tatsuo and Nakamura Eiji. Bilateral master-slave control for manipulators with different configurations. *Journal of the Robotics Society of Japan*, 4(5):469–479, 1986.
- [13] Yosikawa Tuneo. *Foundations of Robotics*, volume 1. The MIT Press, London England, 1990.